

Structural evaluation of three 2-phenylpyrazolo[4,3-c]quinolin-3-one monohydrates



Vitor F. Ferreira^{a,b}, Katia Z. Leal^{a,c}, Eric B. Lindgren^a, Mara R.P. de Oliveira^{a,b}, Maria Celia B.V. de Souza^{a,b}, Thatyana R.A. Vasconcelos^{a,b}, James L. Wardell^{d,e,*}, Solange M.S.V. Wardell^f, Julliane D. Yoneda^g

^a Programa de Pós-Graduação em Química, Instituto de Química, Universidade Federal Fluminense, Outeiro de São João Batista s/n°, 24020-141 Niterói, RJ, Brazil

^b Departamento de Química-Orgânica, Instituto de Química, Universidade Federal Fluminense, Outeiro de São João Batista s/n°, 24020-141 Niterói, RJ, Brazil

^c Departamento de Físico-Química, Instituto de Química, Universidade Federal Fluminense, Outeiro de São João Batista s/n°, 24020-141 Niterói, RJ, Brazil

^d Department of Chemistry, University of Aberdeen, Old Aberdeen AB 24 3UE, Scotland, United Kingdom

^e Instituto de Tecnologia em Fármacos-Farmanginhos, FioCruz – Fundação Oswaldo Cruz, R. Sizenando Nabuco, 100, Mangueiras, Rio de Janeiro, RJ 21041-250, Brazil

^f CHEMSOL, 1 Harcourt Road, Aberdeen AB15 5NY, Scotland, United Kingdom

^g Departamento de Química, Instituto de Ciências Exatas, Universidade Federal Fluminense, Rua Des. Ellis Hermydio Figueira 783, 27213-415 Volta Redonda, RJ, Brazil

HIGHLIGHTS

- M06-2X/6-311++G(d,p) level calculations on structures and tautomeric stabilities of 2-phenylpyrazolo[4,3-c]quinolin-3-ones.
- X-ray crystallographic study of 2-phenylpyrazolo[4,3-c]quinolin-3-one monohydrates.
- Supramolecular arrangements of 2-phenylpyrazolo[4,3-c]quinolin-3-one monohydrates.

ARTICLE INFO

Article history:

Received 4 May 2013

Received in revised form 14 August 2013

Accepted 15 August 2013

Available online 20 August 2013

Keywords:

Pyrazolo[4,3-c]quinolin-3-one

Tautomers

X-ray structure determination

Ab initio calculations

ABSTRACT

A single crystal X-ray diffraction and theoretical study has been carried out on mono hydrates of three 2H-pyrazolo[4,3-c]quinolin-3(5H)-one derivatives, namely 6-methyl-2-phenylpyrazolo[4,3-c]quinolin-3-one, **3**, 6-methyl-2-(4-chlorophenyl)pyrazolo[4,3-c]quinolin-3-one, **4**, and 8-methyl-2-(4-nitrophenyl)pyrazolo[4,3-c]quinolin-3-one, **5**. The monohydrates were obtained on recrystallization from moist solvents. While there are three tautomeric forms possible for such pyrazolo[4,3-c]quinolin-3-one molecules, the sole form isolated in the solid [(X):(H₂O)] (X = **3**, **4** and **5**) compounds was the quinoloid form – the one calculated to be the most stable at the M06-2X/6-311++G(d,p) level of theory. Excellent agreement was found between the calculated and X-ray determined structures. Molecule **5** in [(5):(H₂O)] is very near planar while both molecules **3** and **4** in their respective hydrates are much less so as a consequence of angles about 24° between the two aromatic rings. In each hydrate, the pyrazolo[4,3-c]quinolin-3-one molecule is bonded to three water molecules and each water molecule is likewise H-bonded to three pyrazolo[4,3-c]quinolin-3-one molecules. While the water molecules are H-bonded to **3** and **4** via the pyridinyl N and 2x the carbonyl O atoms, in [(5):(H₂O)] the H-bonds are to pyridinyl N, carbonyl O and a nitro O atoms. Calculations indicated that the found arrangement in [(5):(H₂O)] is more stable than one using the connections as found in [(3):(H₂O)] and [(4):(H₂O)]. While each of the hydrates possess strong N–H···O and O–H···O hydrogen bonds, and weaker C–H···π and π···π interactions, the supramolecular arrays are very different.

© 2013 Elsevier B.V. All rights reserved.

1. Introduction

Pyrazole derivatives exhibit anti-bacterial, anti-inflammatory, hypotensive and anti-tumor activities [1]. In particular, pyrazoles fused with other heterocyclic systems have been found to possess important biological activities, e.g., pyrazolo[3,4-b]quinoline deriv-

atives have anti-viral [2] and anti-malarial [3] activities, while 2-phenylpyrazolo[4,3-c]quinolin-3-ones show anti-viral activities [1,4]: they are also potent antagonists for benzodiazepine receptors [5–7].

The 2-phenylpyrazolo[4,3-c]quinolin-3-ones can exist, theoretically at least, in three tautomeric forms, **I**, **II** and **III**, see Fig. 1, with each form possessing different donor groups and thus different potential for binding to receptor molecules. The most thermodynamically favoured form is **I** in aqueous solutions, as calculated by Karolak-Wojciechowska et al. using the semi-empirical method

* Corresponding author at: Department of Chemistry, University of Aberdeen, Old Aberdeen AB 24 3UE, Scotland, United Kingdom. Tel.: +44 1224 312 819.

E-mail address: j.wardell@abdn.ac.uk (J.L. Wardell).

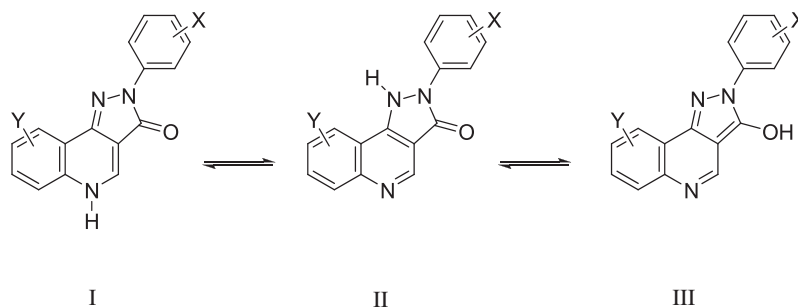


Fig. 1. Tautomeric forms of 2-phenylpyrazolo[4,3-c]quinolin-3-ones.

AM1 from the MOPAC-93 program [7]. This form is also considered the effective form by various groups working on benzodiazepine receptors [8]. A search of the Cambridge Structural Database in April, 2013 revealed that the structures of only two 2-pyrazolo[3,4-b]quinoline derivatives, namely 2-phenyl-2,5-dihydropyrazolo[4,3-c]-3(3H)-one (1) and 2-(4-chlorophenyl)-2,5-dihydropyrazolo[4,3-c]-3(3H)-one (2), both in tautomeric form I, had been reported [9].

As 2-phenylpyrazolo[4,3-c]quinolin-3-ones comprise an important group of compounds and as we had access to some derivatives from an earlier anti-viral activity study [4], we have carried out structure determinations.

The low solubility of 6-methyl- and 8-methyl-2-(XC₆H₄)-2H-pyrazolo[4,3-c]quinolin-3(5H)-ones in organic solvents and the poor quality of crystals obtained were severely restricting. However, suitable crystals for single crystal X-ray studies were obtained on recrystallization of: 6-methyl- 2-phenylpyrazolo[4,3-c]quinolin-3-one, **3**, from moist DMSO, 6-methyl-2-(4-chlorophenyl)pyrazolo[4,3-c]quinolin-3-one, **4**, from moist EtOCH₂CH₂-OH, and 8-methyl- 2-(4-nitrophenyl)pyrazolo[4,3-c]quinolin-3-one, **5**, from moist DMSO/EtOAc, see Scheme 1. The crystals obtained in each case were monohydrates, [**3**·(H₂O)], [**4**·(H₂O)], and [**5**·(H₂O)]. While the intermolecular interactions for the hydrates were expected to be much different from those in the anhydrous compounds, **1** and **2** [9], the influence of the hydrate molecules on the tautomeric forms and molecular conformations was unclear. As the activity of these compounds is of paramount importance in biological media, knowledge of the molecular conformations found in the hydrates could be of considerable value. The crystal structures of these hydrates, as well as theoretical calculations at the M06-2X/6-311++G(d,p) level, are now reported.

2. Experimental

2.1. General

Melting points were determined on a Fisher-Johns apparatus and are uncorrected. Infrared spectra were recorded on a Perkin-Elmer 1420 spectrometer in KBr discs. NMR spectra were recorded on a Varian Unity Plus 300 spectrometer DMSO-*d*₆ solutions. Reactions were monitored by thin-layer chromatography on silica-gel pre-coated F₂₅₄ Merck plates.

2.2. Synthesis

Following well-reported methods [4,10], the 2-phenylpyrazolo[4,3-c]quinolin-3-ones were prepared from successive reactions of diethyl ethoxymethylenemalonate with a toluidine, thionyl chloride (20 mL) and an arylhydrazine.

2.2.1. 8-Methyl-2-phenyl-2H-pyrazolo[4,3-c]quinolin-3(5H)-one, **3**

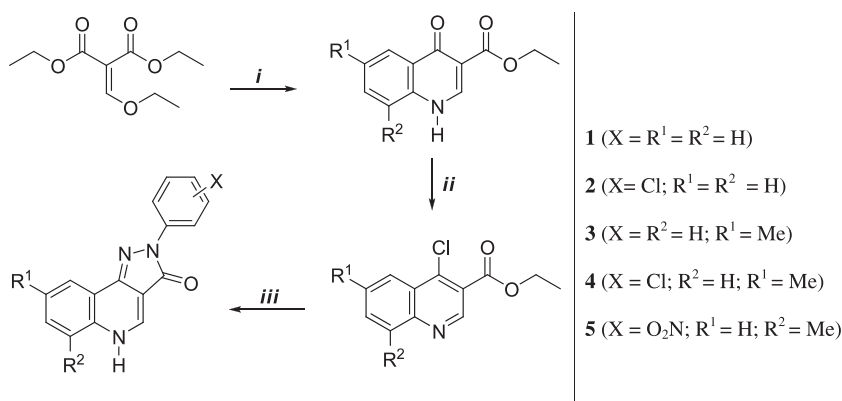
The toluidine and arylhydrazine employed in the synthesis were 4-toluidine and phenylhydrazine. The crystal used in the structure determination was grown from moist DMSO/EtOAc as the monohydrate.

m.p.: 308–309 °C.

¹H NMR [300.00 MHz, DMSO-*d*₆] δ: 12.75 (1H; s; NH); 8.73 (1H; d; *J* = 6.3 Hz; H₄); 8.37–8.32 (2H; m; H₂); 8.15 (1H; s; H₉); 7.73 (1H; d; *J* = 8.4 Hz; H₆); 7.72–7.52 (3H; m; H₇ and H₃); 7.31–7.25 (1H; m; H₄); 2.60 (3H, s; CH₃) ppm.

¹³C NMR [75.0 MHz, DMSO-*d*₆] δ: 161.8; 143.1; 140.3; 138.9; 136.4; 133.6; 131.5; 128.8; 124.0; 121.7; 119.5; 118.8; 118.7; 106.0; 21.0 ppm.

IR (cm⁻¹; KBr): ν_{max} 3300–2550 (NH/OH); 1620 (C=O).



Scheme 1. Reagents: (i) R¹R²C₆H₃NH₂, Δ; (ii) SOCl₂, Δ; (iii) XC₆H₄NHNH₂, Δ; AcOH, Δ.

Table 1
Crystal data and structure refinement.

	[3 ·(H ₂ O)]	[4 ·(H ₂ O)]	[5 ·(H ₂ O)]
Empirical formula	C ₁₇ H ₁₅ N ₃ O ₂	C ₁₇ H ₁₄ ClN ₃ O ₂	C ₁₇ H ₁₄ N ₄ O ₄
Formula weight	293.32	327.76	338.32
Temperature (K)	120(2)	120(2)	3120(2)
Wavelength (Å)	0.71073	0.6889	0.6889
Crystal system, space group	Orthorhombic, Pbc _a	Orthorhombic, Pbc _a	Monoclinic, P2 ₁ /n
Unit cell dimensions			
<i>a</i> (Å)	12.0115(8)	35.11(6)	4.706(2)
<i>b</i> (Å)	6.9719(4)	12.34(2)	27.273(13)
<i>c</i> (Å)	32.585(2)	6.916(13)	11.546(6)
β (°)			97.449(5)
Volume (Å ³)	2728.8(3)	2996(9)	1469.5(12)
<i>Z</i>	8	8	4
Density (calculated) (Mg/m ³)	1.428	1.453	1.529
Absorption coefficient (mm ⁻¹)	0.096	0.269	0.112
<i>F</i> (000)	1232	1360	704
Crystal size (mm ⁻¹)	0.5 × 0.06 × 0.02	0.08 × 0.04 × 0.01	0.06 × 0.02 × 0.01
Theta range for data collection (°)	3.02–27.49	1.12–24.27°	1.87–31.79
Index ranges	–14 ≤ <i>h</i> ≤ 15 –9 ≤ <i>k</i> ≤ 8 –42 ≤ <i>l</i> ≤ 37	–38 ≤ <i>h</i> ≤ 41 –14 ≤ <i>k</i> ≤ 14 –8 ≤ <i>l</i> ≤ 8	–6 ≤ <i>h</i> ≤ 4 –40 ≤ <i>k</i> ≤ 41 –16 ≤ <i>l</i> ≤ 17
Reflections collected	17,601	22,320	19,127
Independent reflections	3078 [<i>R</i> (int) = 0.1685]	2639 [<i>R</i> (int) = 0.0612]	4902 [<i>R</i> (int) = 0.0477]
Reflections observed (>2σ)	1305	2157	3815
Data completeness	0.99	0.99	0.9
Absorption correction	Multi-scans	Multi-scans	Multi-scans
Max. and min. transmission	0.7456 and 0.5653	0.860 and 1.000	0.882 and 1.000
Refinement method	Full-matrix least-squares on <i>F</i> ²	Full-matrix least-squares on <i>F</i> ²	Full-matrix least-squares on <i>F</i> ²
Data/restraints/parameters	3078/0/209	2639/3/215	4902/0/236
Goodness-of-fit on <i>F</i> ²	0.976	1.134	1.067
Final <i>R</i> indices [<i>I</i> > 2σ(<i>I</i>)]	<i>R</i> ₁ = 0.081 <i>wR</i> ₂ = 0.163	<i>R</i> ₁ = 0.044 <i>wR</i> ₂ = 0.107	<i>R</i> ₁ = 0.062 <i>wR</i> ₂ = 0.149
<i>R</i> indices (all data)	<i>R</i> ₁ = 0.207 <i>wR</i> ₂ = 0.218	<i>R</i> ₁ = 0.059 <i>wR</i> ₂ = 0.125	<i>R</i> ₁ = 0.084 <i>wR</i> ₂ = 0.165
Largest diff. peak and hole (eÅ ⁻³)	0.354 and –0.338	0.235 and –0.291	0.377 and –0.326

Table 2

Energies of the tautomeric forms of 2-phenylpyrazolo[4,3-*c*]quinolin-3-ones calculated using the Gaussian 09W program, at the M06-2X/6-311++G(d,p) level of theory [11].

Compound	I	II	III
(a) Gibbs free energies (kcal mol ⁻¹)			
3	–561476.7	–561473.3	–561468.8
4	–849888.2	–849884.5	–849880.1
5	–689799.1	–689794.9	–689788.9
(b) Relative energies (kcal mol ⁻¹)			
ΔG (kcal mol ⁻¹)	3	4	5
$\Delta(I-II)$	–3.4	–3.7	–4.2
$\Delta(I-III)$	–7.9	–8.1	–10.2

2.2.2. 2-(4-Chlorophenyl)-8-methyl-2H-pyrazolo[4,3-*c*]quinolin-3(5H)-one, **4**

The toluidine and arylhydrazine employed in the synthesis were 4-toluidine and 4-chlorophenylhydrazine. The crystal used in the structure determination was grown from moist EtOCH₂CH₂-OH as the monohydrate.

m.p.: 272–273 °C.

¹H NMR [300.00 MHz, DMSO-*d*₆] δ : 12.95 (1H; s; NH); 8.82 (1H; d; *J* = 6.6 Hz; H₄); 8.38 (2H; d; *J* = 9.0 Hz; H₂); 8.14 (1H; s; H₉); 7.73 (1H; d; *J* = 8.7 Hz; H₆); 7.61 (2H; d; *J* = 9.0 Hz; H₃); 7.50 (1H; dd; *J* = 8.4 and 2.1 Hz; H₇); 2.60 (3H; s; CH₃) ppm.

¹³C NMR [75.0 MHz, DMSO-*d*₆] δ : 161.8; 143.4; 139.1; 139.0; 136.4; 133.6; 131.6; 128.7; 127.7; 121.7; 120.0; 119.5; 118.6; 105.7; 21.0 ppm.

IR (cm⁻¹; KBr): ν_{\max} 3680–2500 (NH/OH); 1620 (C=O).

2.2.3. 6-Methyl-2-(4-nitrophenyl)-2H-pyrazolo[4,3-*c*]quinolin-3(5H)-one, **5**

The toluidine and arylhydrazine employed in the synthesis were 2-toluidine and 4-nitrophenylhydrazine. The crystal used in the structure determination was grown from moist EtOCH₂CH₂OH as the monohydrate.

m.p.: 278–280 °C.

IR (cm⁻¹; KBr pellets): ν_{\max} 3600–2500 (NH/OH); 1650 (C=O).

2.3. Calculations

The calculations on the tautomeric forms and aggregates were performed using the Gaussian 09W program [11]. Molecular geometries of each tautomer and each aggregate were initially based on the final experimental structures found in the X-ray study. The tautomers were fully optimized using the M06-2X/6-311++G(d,p) level of theory. Since no imaginary frequency was found, all the optimized structures were characterized as minima energy structures. In the case of the aggregates, a single point calculation were performed using the same level of theory.

2.4. Crystallography

Data for [**3**·(H₂O)] were obtained at 120(2) K with Mo K α radiation, λ = 0.71073 Å, by means of the Bruker–Nonius 95 mm CCD camera on kappa gonistat diffractometer of the EPSRC crystallographic service. Data collection was carried out under the control of the program COLLECT [12] and data reduction and unit cell refinement were achieved with the COLLECT and DENZO [13] programs. Data for [**4**·(H₂O)] and [**5**·(H₂O)] were obtained at 120(2) K

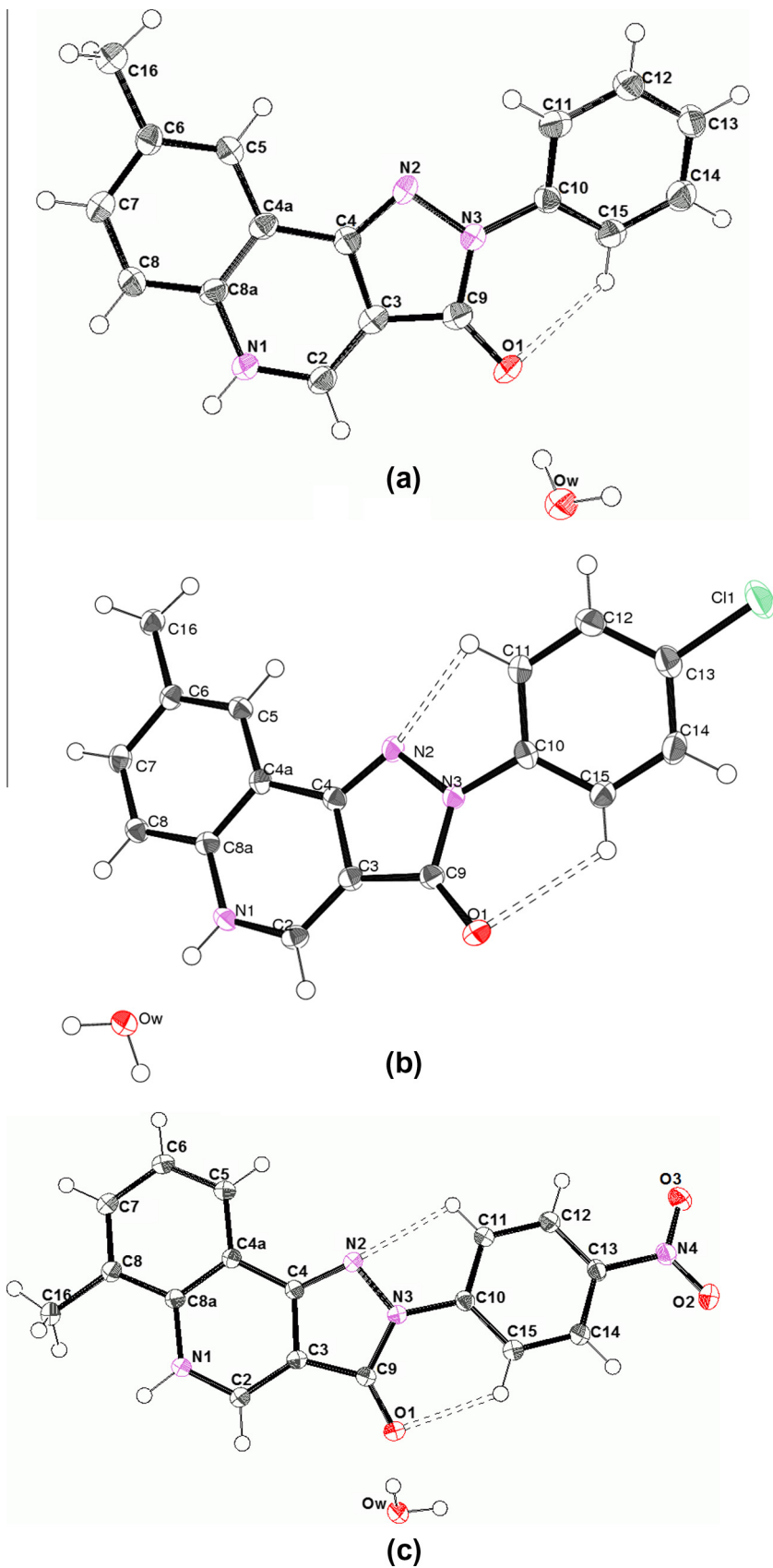


Fig. 2. Atom arrangements and numbering schemes for (a) [3·(H₂O)], (b) [4·(H₂O)] and (c) [5·(H₂O)]. Hydrogen bonds are drawn as dashed lines. Probability ellipsoids are drawn at the 50% level. Hydrogen atoms are drawn as spheres of arbitrary radius.

Table 3
Selected measured and calculated bond angles and lengths, (Å, °).

	[3 ·(H ₂ O)]		[4 ·(H ₂ O)]		[5 ·(H ₂ O)]		1 [9]	2 [9]
	X-ray	Calculated	X-ray	Calculated	X-ray	Calculated	X-ray	X-ray
N(2)—N(3)	1.420(4)	1.39	1.429(3)	1.39	1.4091(17)	1.39	1.412(4)	1.420(5)
N(3)—C(9)	1.376(5)	1.40	1.384(4)	1.40	1.4055(18)	1.40	1.375(4)	1.382(5)
C(9)—C(3)	1.438(5)	1.46	1.453(4)	1.46	1.433(2)	1.46	1.426(4)	1.427(6)
C(3)—C(4)	1.429(5)	1.43	1.441(4)	1.43	1.4261(19)	1.43	1.422(4)	1.430(6)
C(4)—N(2)	1.316(4)	1.29	1.317(4)	1.30	1.3156(19)	1.30	1.312(4)	1.303(5)
C(4)—C(4A)	1.447(5)	1.45	1.454(4)	1.45	1.437(2)	1.45	1.440(4)	1.434(5)
C(4A)—C(8A)	1.404(5)	1.40	1.414(4)	1.40	1.407(2)	1.40	1.398(4)	1.417(4)
C(8A)—N(1)	1.399(5)	1.40	1.409(3)	1.40	1.3991(19)	1.40	1.403(4)	1.404(5)
N(1)—C(2)	1.336(4)	1.35	1.357(3)	1.35	1.3404(19)	1.35	1.323(4)	1.324(5)
C(2)—C(3)	1.360(5)	1.35	1.374(4)	1.35	1.372(2)	1.35	1.364(4)	1.361(6)
C(3)—C(4)	1.429(5)	1.43	1.441(4)	1.43	1.4261(19)	1.43	1.422(4)	1.430(6)
O(1)—C(9)	1.268(4)	1.22	1.275(3)	1.22	1.2410(18)	1.22	1.252(3)	1.250(5)
C(13)—Cl			1.746(4)	1.74				1.739(4)
N(2)—C(4)—C(3)	112.8(4)	112.5	112.9(2)	112.5	113.28(13)	112.5	113.9(2)	113.0(3)
C(4)—C(3)—C(9)	105.6(3)	105.8	106.0(2)	105.9	106.31(13)	105.9	106.3(2)	105.8(4)
C(3)—C(9)—N(3)	103.8(3)	102.1	103.0(2)	102.0	102.89(12)	102.0	103.3(2)	103.9(4)
C(9)—N(3)—N(2)	113.7(3)	113.7	114.25(18)	113.8	113.55(12)	113.7	113.9(2)	113.05(3)
N(3)—N(2)—C(4)	103.6(3)	105.9	103.78(18)	105.8	103.97(11)	105.8	103.6(2)	104.2(3)

with Synchrotron radiation, $\lambda = 0.68890$ Å, by means of the Rigaku Saturn724+ (2×2 bin mode) of the EPSRC crystallographic service. Data collection, data reduction and unit cell refinement were achieved with the CrystalClear program [14].

Correction for absorption was achieved in each case by a semi-empirical method based upon the variation of equivalent reflections with the program SADABS 2007/2 [15] for [**3**·(H₂O)] and CrystalClear program [14] for [**4**·(H₂O)] and [**5**·(H₂O)]. The programs ORTEP-3 for Windows [16] and MERCURY [17] were used in the preparation of the figures. SHELXL97 [18] and PLATON [19] were used in the calculation of molecular geometry. The structures were solved by direct methods using SHELXS-97 [18] and fully refined by means of the program SHELXL-97 [18]. Difference map peaks provided positions for the hydrogen atoms of the NH groups and of water molecules for which the coordinates, along with isotropic displacement parameters, were fully refined. All other hydrogen atoms were placed in calculated positions. Crystal data and structure refinement details are listed in Table 1.

3. Results and discussion

3.1. Synthesis

The synthesis of the 2-phenylpyrazolo[4,3-*c*]quinolin-3-one compounds is shown in Scheme 1. The crystals obtained in each case after recrystallization were monohydrates, [**3**·(H₂O)], obtained from moist DMSO [**4**·(H₂O)], from moist EtOCH₂CH₂OH and [**5**·(H₂O)] recrystallized from moist DMSO/EtOAc.

3.2. Tautomer stability

Calculations on the tautomeric forms were performed using the Gaussian 09W program, at the M06-2X/6-311++G(d,p) level of theory [11]. As shown in Table 2, for each of **3–5**, the most stable form is **I** and the least stable form is **III**. This finding of the most stable tautomer concurs with that found by Karolak-Wojciechowska et al. using the semi-empirical method AM1 in the MOPAC-93 program [7].

3.3. Crystallography

The asymmetric unit consists in each case of a molecule of a single molecule of a 2-phenylpyrazolo[4,3-*c*]quinolin-3-one derivative and a hydrate molecule.

3.3.1. Molecular structures

Fig. 2 shows the atom arrangements and numbering schemes for [**3**·(H₂O)], [**4**·(H₂O)] and [**5**·(H₂O)]. Selected bond lengths and angles associated with the pyrazole rings in [**3**·(H₂O)], [**4**·(H₂O)] and [**5**·(H₂O)] are listed in Table 3, as are the experimental values for **1** and **2** [9]. The only significant difference between the geometric parameters for the hydrates and the anhydrous analogues involves the C=O bond lengths, which are longer in the hydrates due to their involvement in hydrogen bonding to the solvate molecules. Theoretical values for each lowest energy tautomer, calculated at the M06-2X/6-311++G(d,p) level of theory, are also listed with the experimental values. As can be seen the experimental values for [**3**·(H₂O)], [**4**·(H₂O)] and [**5**·(H₂O)] are close to the calculated values for **3**, **4** and **5**.

Molecules of **3–5** in the hydrates exist in the tautomeric form **I**, see Fig. 1. Overall, molecule **5** in [**5**·(H₂O)] is very near planar, with the angle between the pyrazolo[4,3-*c*]quinolin-3-one and the nitrophenyl rings of 7.40 (8)°; furthermore the nitro group is only 3.6 (3)° out of the plane of its attached phenyl ring. Molecules **3** and **4** deviate much more severely from planarity as indicated by the 23.56(8)° and 24.85(0.12)° angles, respectively, between the pyrazolo[4,3-*c*]quinolin-3-one and the phenyl moieties.

The PLATON program [19] reveals the presence of C15—H15···O1 intramolecular hydrogen bonds in **3–5**, with additionally intramolecular hydrogen bonds, C11—H11···N2, present in **4** and **5**, see Table 4: in **3**, the H11···N2 separation is just beyond the cut-off value of 2.50 Å and at best this indicates a very weak interaction. The chloro and nitro groups in **4** and **5**, being electron withdrawing groups, will render the attached ring hydrogens more positive and hence more acceptable to involvement in hydrogen bonding than those in **3**. There is a difference in the conformations of **3** and **4**, on one hand, and **5**, on the other, as shown by the orientations of the C1—C6 phenyl ring: this is indicated by the N2—N3—C10—C11 torsion angles of 22.6(5)°, 22.1(3)° and −3.3(2)° for **3–5**, respectively. The corresponding values for the anhydrous compounds **1** and **2** were reported to be −41.2(4)° and 10.2(5)° [9]. The presence of the methyl group in **3–5** is not considered to have an influence on these torsion angles.

3.3.2. Crystal structures

Each of the three hydrates possess strong N—H···O and O—H···O hydrogen bonds, and weaker C—H··· π [20] and π ··· π interactions [21], see Table 4. In addition, there are weak C—H···Cl hydrogen bonds [22] in [**4**·(H₂O)] and C—H···O hydrogen bonds in [**5**·(H₂O)]. Despite most of the strong intermolecular interactions

Table 4
Geometric parameters (Å, °) for the intra- and inter-molecular interactions.

Compound	D—H...A	D—H	H...A	D...A	D—H...A		
<i>(a) Intramolecular hydrogen bonds</i>							
[3·(H ₂ O)]	C(15)—H(15)...O(1)	0.93	2.40	2.958(5)	118		
[4·(H ₂ O)]	C(15)—H(15)...O(1)	0.93	2.53	3.051(6)	116		
[4·(H ₂ O)]	C(11)—H(11)...N(2)	0.93	2.42	2.753(6)	101		
[5·(H ₂ O)]	C(11)—H(11)...N(2)	0.93	2.38	2.731(3)	102		
[5·(H ₂ O)]	C(15)—H(15)...O(1)	0.93	2.25	2.890(3)	125		
<i>(b) Intermolecular hydrogen bonds</i>							
[3·(H ₂ O)]	N(1)—H(1)...OW ^{iv}	0.88(4)	1.83(4)	2.707(4)	178(5)		
[3·(H ₂ O)]	OW—HW(1)...O(1) ^v	0.94(4)	1.80(4)	2.735(4)	175(4)		
[3·(H ₂ O)]	OW—HW(2)...O(1)	0.88(4)	1.90(4)	2.777(4)	175(4)		
[4·(H ₂ O)]	N(1)—H(1)...OW	0.86	1.89	2.742(6)	170		
[4·(H ₂ O)]	OW—HW(1)...O(1) ^{vi}	0.87(3)	1.98(3)	2.841(6)	169(3)		
[4·(H ₂ O)]	OW—HW(2)...O(1) ^{vii}	0.88(3)	1.92(3)	2.794(6)	172(2)		
[4·(H ₂ O)]	C(11)—H(11)...Cl(1) ^{viii}	0.93	2.75	3.568(7)	148		
[5·(H ₂ O)]	N(1)—H(1)...OW ⁱ	0.95(2)	1.87(2)	2.777(2)	157.9(17)		
[5·(H ₂ O)]	OW—HW(1)...O(1)	0.90(3)	1.88(3)	2.770(2)	172(2)		
[5·(H ₂ O)]	OW—HW(2)...O(2) ⁱⁱ	0.89(3)	2.07(3)	2.935(2)	163(2)		
[5·(H ₂ O)]	C(2)—H(2)...O(1) ⁱⁱⁱ	0.93	2.33	3.215(2)	158		
Symmetry operations: i = -x, -y, 2 - z; ii = 2 - x, -y, 1 - z; iii = 1 - x, -y, 2 - z; iv = -1/2 + x, 1/2 - y, -z; v = 1/2 - x, -1/2 + y, z; vi = 1 - x, -1/2 + y, 1/2 - z; vii = 1 - x, 1 - y, 1 - z; viii = 3/2 - x, -1/2 + y, z.							
Compound	C—H...Cg ^a	H...Cg	H _{perp}	γ	C—H...Cg ^a	C...Cg	
<i>(c) C—H...π interactions</i>							
[3·(H ₂ O)]	C(12)—H(12)...Cg(4) ⁱⁱ	2.96	2.80	19.07	126	3.594(4)	
[4·(H ₂ O)]	C(12)—H(12)...Cg(4) ⁱⁱⁱ	2.85	2.81	9.76	153	3.703(8)	
[5·(H ₂ O)]	C(16)—H(16B)...Cg(2) ⁱ	2.72	2.68	9.98	129	3.412(3)	
Compound	Cg(1)...Cg(J) ^a	Cg...Cg	α	β	γ	Cg(I) _{perp}	Cg(J) _{perp}
<i>(d) π...π intermolecular contacts</i>							
[3·(H ₂ O)]	Cg(1)...Cg(3) ⁱⁱⁱ	3.605(2)	1.55(18)	17.35	18.48	3.4195(14)	3.4411(14)
[3·(H ₂ O)]	Cg(2)...Cg(2) ⁱⁱⁱ	3.781(2)	0	22.68	23.79	3.4603(14)	3.4887(14)
[3·(H ₂ O)]	Cg(2)...Cg(3) ⁱⁱⁱ	3.631(2)	1.06(16)	18.59	17.56	3.4622(14)	3.4416(14)
[3·(H ₂ O)]	Cg(3)...Cg(1) ⁱⁱⁱ	3.887(2)	1.55(18)	24.62	25.64	3.5038(14)	3.5331(14)
[3·(H ₂ O)]	Cg(3)...Cg(2) ⁱⁱⁱ	3.625(2)	1.06(16)	15.65	14.62	3.5075(14)	3.4901(14)
[3·(H ₂ O)]	Cg(1)...Cg(3) ^{iv}	3.887(2)	1.55(18)	25.64	24.62	3.5331(14)	3.5040(14)
[3·(H ₂ O)]	Cg(2)...Cg(2) ^{iv}	3.782(2)	0	23.79	22.68	3.4890(14)	3.4605(14)
[3·(H ₂ O)]	Cg(2)...Cg(3) ^{iv}	3.625(2)	1.06(16)	14.62	15.65	3.4904(14)	3.5077(14)
[3·(H ₂ O)]	Cg(3)...Cg(1) ^{iv}	3.605(2)	1.55(18)	18.48	17.35	3.4413(14)	3.4195(14)
[3·(H ₂ O)]	Cg(3)...Cg(2) ^{iv}	3.632(2)	1.06(16)	17.56	18.59	3.4419(14)	3.4625(14)
[4·(H ₂ O)]	Cg(1)...Cg(3) ^v	3.564(7)	1.20(11)	15.74	16.87	3.4106(9)	3.4303(8)
[4·(H ₂ O)]	Cg(2)...Cg(2) ^v	3.732(7)	0	22.71	22.93	3.4367(8)	3.4424(8)
[4·(H ₂ O)]	Cg(2)...Cg(3) ^v	3.657(7)	0.27(10)	20.14	19.96	3.4377(8)	3.4338(8)
[4·(H ₂ O)]	Cg(3)...Cg(1) ^v	3.866(7)	1.20(11)	26.10	27.18	3.4388(8)	3.4717(9)
[4·(H ₂ O)]	Cg(3)...Cg(2) ^v	3.598(7)	0.27(10)	16.77	16.74	3.4452(8)	3.4446(8)
[4·(H ₂ O)]	Cg(1)...Cg(3) ^{vi}	3.866(7)	1.20(11)	27.18	26.10	3.4717(9)	3.4388(8)
[4·(H ₂ O)]	Cg(2)...Cg(2) ^{vi}	3.732(7)	0	22.93	22.71	3.4423(8)	3.4366(8)
[4·(H ₂ O)]	Cg(2)...Cg(3) ^{vi}	3.598(7)	0.27(10)	16.74	16.77	3.4446(8)	3.4452(8)
[4·(H ₂ O)]	Cg(3)...Cg(1) ^{vi}	3.564(7)	1.20(11)	16.87	15.74	3.4303(8)	3.4106(9)
[4·(H ₂ O)]	Cg(3)...Cg(2) ^{vi}	3.657(7)	0.27(10)	19.96	20.14	3.4338(8)	3.4377(8)
[5·(H ₂ O)]	Cg(1)...Cg(2) ⁱ	3.517(2)	3.517(2)	21.01	20.74	3.2889(6)	3.2831(6)
[5·(H ₂ O)]	Cg(1)...Cg(3) ⁱ	3.819(2)	2.30(8)	28.50	30.25	3.2987(6)	3.3560(6)
[5·(H ₂ O)]	Cg(4)...Cg(1) ⁱ	3.517(2)	6.19(8)	20.34	14.47	3.4053(7)	3.2974(6)
[5·(H ₂ O)]	Cg(1)...Cg(4) ⁱⁱ	3.517(2)	6.19(8)	14.47	20.34	3.2974(6)	3.4053(7)
[5·(H ₂ O)]	Cg(2)...Cg(1) ⁱⁱ	3.517(2)	1.10(8)	20.74	21.01	3.2831(6)	3.2889(6)
[5·(H ₂ O)]	Cg(3)...Cg(1) ⁱⁱ	3.819(2)	2.30(8)	30.25	28.50	3.3559(7)	3.2988(6)

Cg1—Cg4 are the centroids of the [N(2), N(3), C(9), C(3), C(4)], [N(1), C(2)—C(4), C(5a), C(8a)], [C(4a), C(11)—C(8), C(8a)] and [C(10)—C(15)] rings, respectively; Alpha is the dihedral angle between the least squares planes of the overlapping rings. Beta is the angle between the vectors Cg...Cg and Cg(I)_{perp} where Cg(I)_{perp} is the perpendicular distance of Cg(I) from the plane of ring J. Similarly gamma is the angle between the vectors Cg...Cg and Cg(J)_{perp}.

Symmetry codes: i = 1 + x, y, z; ii = -1 - x, y, z; iii = -1/2 - x, -1/2 + y, z; iv = -1/2 - x, 1/2 + y, z; v = x, 1/2 - y, -1/2 + z; vi = x, 1/2 - y, 1/2 + z.

^a Cg(2) and Cg(4) are the centroids of the [N(2), N(3), C(9), C(3), C(4)] and [C(10)—C(15)] rings, respectively; gamma is the angle at H between the vectors X...Cg and X_{perp}. Symmetry operations: i = -1 + x, y, z; ii = -x, -1/2 + y, 1/2 - z; iii = 3/2 - x, 1 - y, -1/2 + z.

being common to the three hydrates, significant differences in the supramolecular arrays are met.

To facilitate discussions of the intermolecular interactions, the interactions are divided into sub-sets. The first sub-set to be considered involves the strong classical N—H...O and O—H...O hydrogen bonds. In each of [3·(H₂O)], [4·(H₂O)] and [5·(H₂O)], the hydrate molecules are hydrogen bonded to three 2-phenylpyrazol-

o[4,3-c]quinolin-3-one molecules via one N—H...O and two O—H...O hydrogen bonds, and each of the phenylpyrazolo[4,3-c]quinolin-3-one molecules is likewise hydrogen-bonded to three hydrate molecules, see Fig. 3. The summations of the angles about the hydrate oxygen atom in [3·(H₂O)], [4·(H₂O)] and [5·(H₂O)] are 358.2°, 356.4° and 347.7°, respectively, indicating a progressive distortion away from planarity.

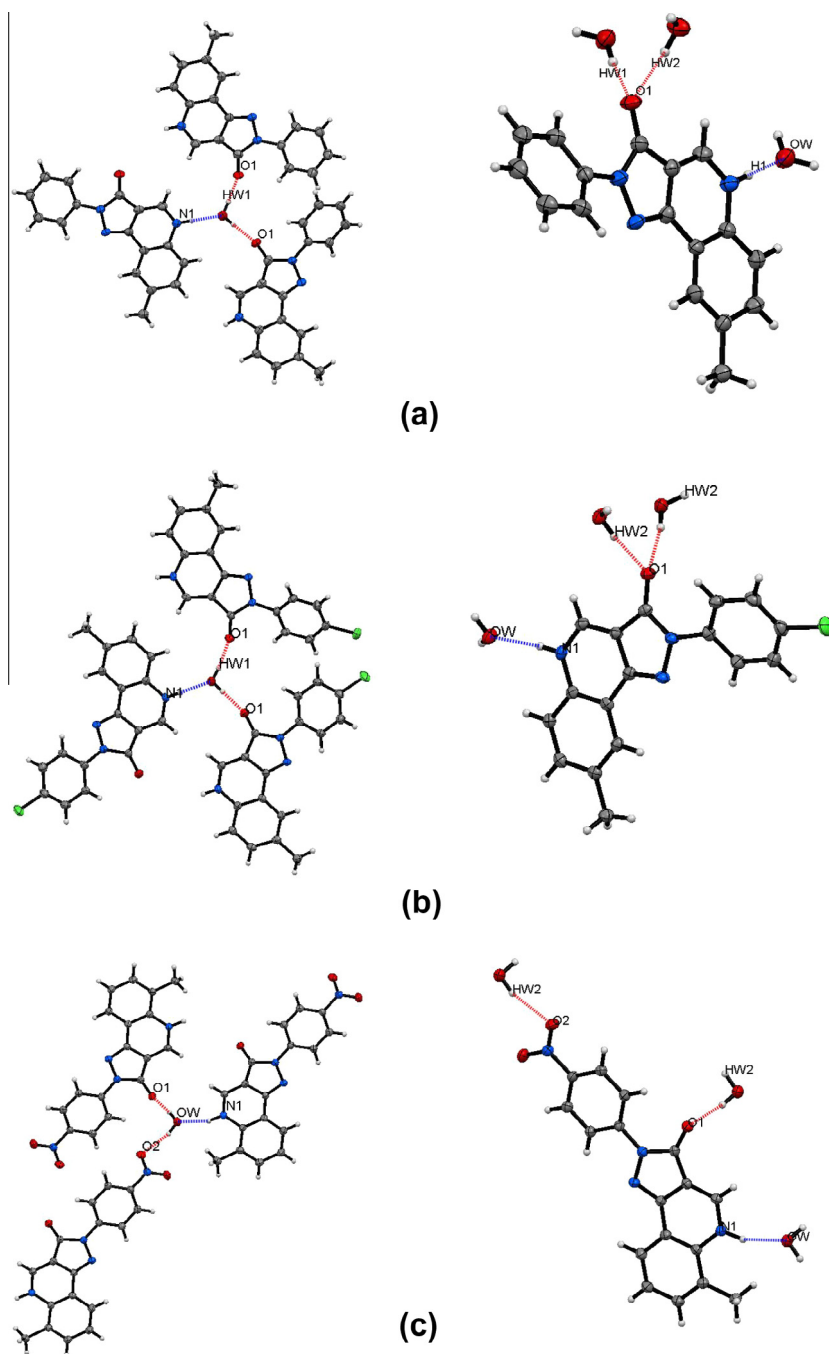


Fig. 3. Arrangements around the hydrate molecules and the direct interactions of the hydrate molecules with 2-phenylpyrazolo[4,3-c]quinolin-3-ones in (a) [3·(H₂O)], (b) [4·(H₂O)] and (c) [5·(H₂O)].

There are differences in the arrangements of the three phenylpyrazolo[4,3-c]quinolin-3-one molecules about the hydrate molecules. In both [3·(H₂O)] and [4·(H₂O)] the carbonyl oxygen of the phenylpyrazolo[4,3-c]quinolin-3-one molecules acts as a double acceptor in two hydrogen bonds. While in both [3·(H₂O)] and [4·(H₂O)] the hydrate-phenylpyrazolo[4,3-c]quinolin-3-one interactions involve N1–H1···OW, OW–HW1···O1 and OW–HW2···O1 hydrogen bonds [O1 is the carbonyl oxygen], the orientations of the molecule, hydrogen-bonded via N1, are different, and arise from rotations by 180° about the N1–H1 bond, compare Fig. 3a and b. This rotation of the phenylpyrazolo[4,3-c]quinolin-3-one molecule within the [4]₃·(H₂O) moiety is considered to allow better packing in the crystal.

A more distinct difference is found with [5·(H₂O)]: here the hydrogen bonds connecting the water molecule to the three phenylpyrazolo[4,3-c]quinolin-3-one molecules are N1–H1···OW, OW–HW1···O1 and OW–HW2···O2 hydrogen bonds, where O2 is a nitro group oxygen and O1 is the carbonyl oxygen, see Fig. 3c. Consequently, there are differences in the intermolecular arrays produced by [3·(H₂O)], [4·(H₂O)] and [5·(H₂O)]. Table 3 lists the symmetry operations and geometric parameters of the intermolecular interactions.

In [3·(H₂O)], extended combinations of the N1–H1···OW, OW–HW1···O1 and OW–HW2···O1 hydrogen bonds generate a complex array, as partially exemplified in Fig. 4: for reasons of clarity, not all the possible N1–H1···OW, OW–HW1···O1 and

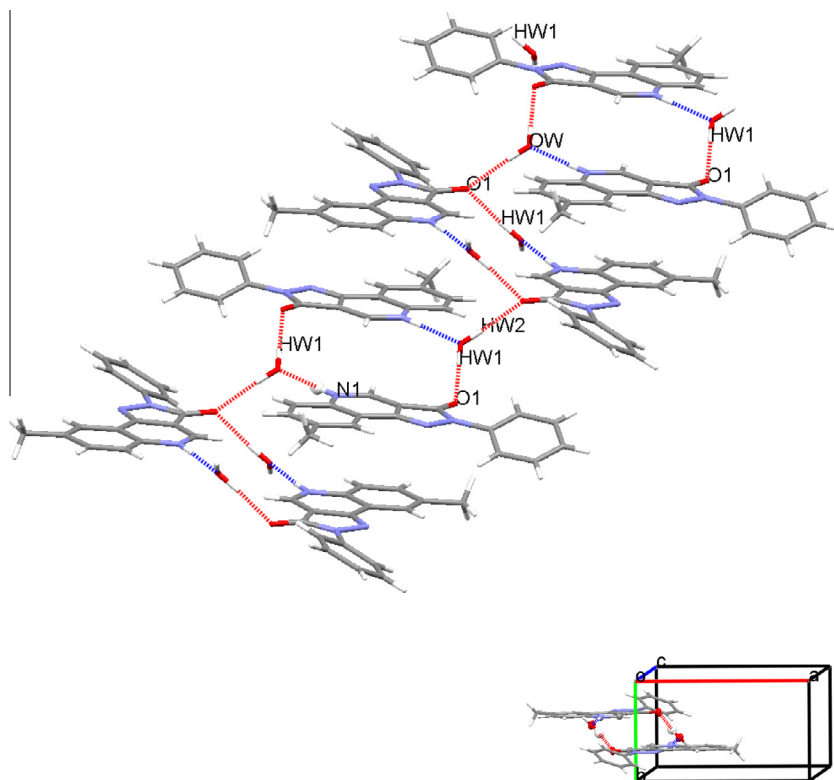


Fig. 4. Compound $[3 \cdot (H_2O)]$. A double chain of molecules of **3** and water molecules formed from combinations of $N1-H1 \cdots OW$, $OW-HW1 \cdots O1$ and $OW-HW2 \cdots O1$ hydrogen bonds. The $N-H \cdots O$ and $O-H \cdots O$ hydrogen bonds are drawn as blue and red green dashed lines respectively. The inset is a view looking down the superimposed chains. Table 4 lists the symmetry operations, and geometric parameters for the intermolecular interactions. (For interpretation of the references to colour in this figure legend, the reader is referred to the web version of this article.)

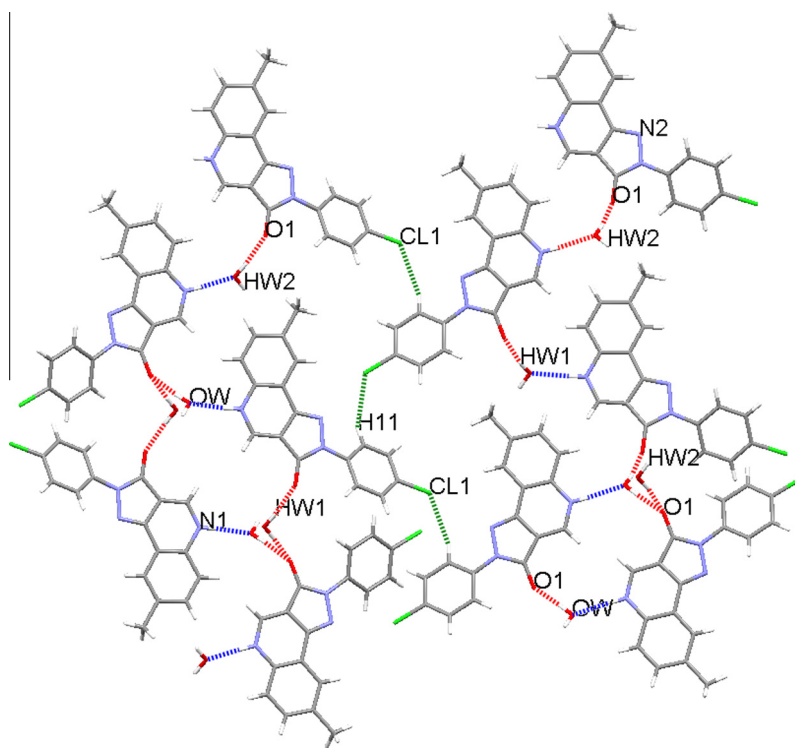


Fig. 5. Compound $[4 \cdot (H_2O)]$. A partial network of molecules of **4** and water generated from $N1-H1 \cdots OW$, $OW-HW \cdots O1$, $OW-HW2 \cdots O1$ and $C11-H11 \cdots Cl1$ hydrogen bonds. The $N-H \cdots O$, $O-H \cdots O$ and $C-H \cdots Cl$ hydrogen bonds are drawn as blue, red and green dashed lines respectively. Table 4 lists details of the symmetry operations and geometric parameters for the intermolecular hydrogen bonds. (For interpretation of the references to colour in this figure legend, the reader is referred to the web version of this article.)

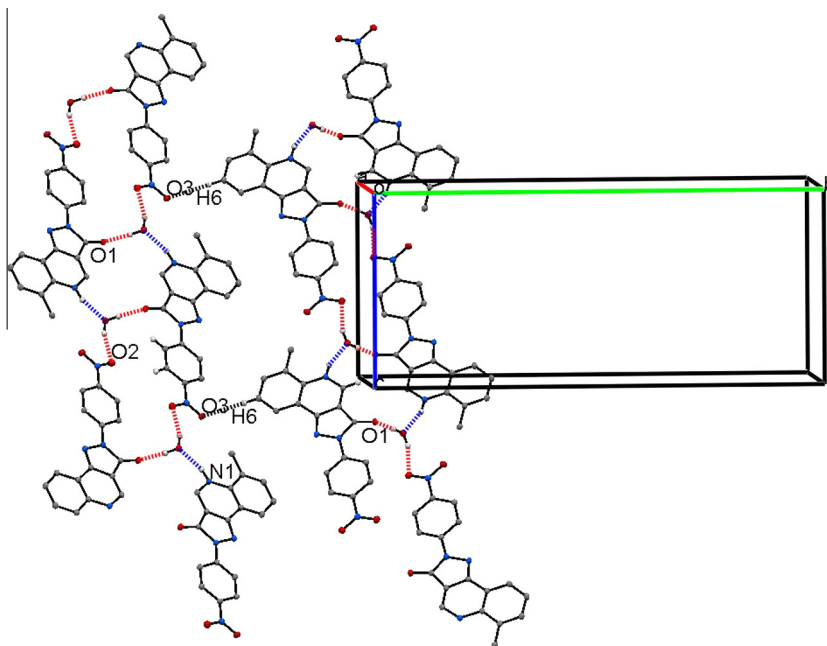


Fig. 6. $[5 \cdot (\text{H}_2\text{O})]$. Alternating centrosymmetric rings, $R_4^4(24)$ and $R_4^4(16)$, formed between double chains, $C_2^2(14)$, of alternating hydrate and molecules **5**, generated from $\text{N1-H1} \cdots \text{OW}$ [blue dash lines], $\text{OW-HW1} \cdots \text{O1}$ and $\text{OW-HW2} \cdots \text{O2}$ hydrogen bonds [both red dashed lines]. The short contacts between the double chains, involving H6-O3 , [$\text{H6-O3} = 2.61 \text{ \AA}$] are shown as black dash lines. Hydrogen atoms not involved in the hydrogen bonds have been omitted for clarity. Table 4 lists the symmetry operations and geometric parameters. (For interpretation of the references to colour in this figure legend, the reader is referred to the web version of this article.)

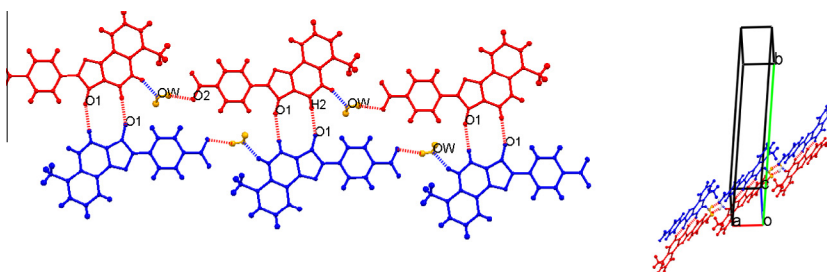


Fig. 7. Compound $[5 \cdot (\text{H}_2\text{O})]$. $\text{C2-H2} \cdots \text{O1}$ interactions link strands of different double chains to generate $R_2^2(10)$ rings, which alternate with $R_6^6(10)$ rings, formed from combinations of $\text{C2-H2} \cdots \text{O1}$, $\text{C1-H1} \cdots \text{OW}$ and $\text{OW-HW2} \cdots \text{O2}$ hydrogen bonds. Molecules in different double chains are drawn in different colours. Table 4 lists the symmetry operation and geometric parameters.

$\text{OW-HW2} \cdots \text{O1}$ hydrogen bonds have been drawn. However, apparent in Fig. 4 are $R_4^4(16)$ rings [23], generated from $\text{N1-H1} \cdots \text{OW}$ and $\text{OW-HW1} \cdots \text{O1}$ hydrogen bonds, and chains, $C_4^4(20)$ [23], generated from $\text{N1-H1} \cdots \text{OW}$ and $\text{OW-HW2} \cdots \text{O1}$ hydrogen bonds. The inset in Fig. 4 is a view looking through the $R_4^4(16)$ rings [23].

In $[4 \cdot (\text{H}_2\text{O})]$, weak $\text{C11-H11} \cdots \text{Cl1}$ hydrogen bonds in combination with the $\text{N1-H1} \cdots \text{OW}$, $\text{OW-HW1} \cdots \text{O1}$ and $\text{OW-HW2} \cdots \text{O1}$ hydrogen-bonds link $\{[(\text{H}_2\text{O})_4]_3\}$ moieties into a complex network of rings and chains, see Fig. 5. Again for reasons of clarity, not all the hydrogen bonds have been drawn. Combinations of $\text{N1-H1} \cdots \text{OW}$, $\text{OW-HW1} \cdots \text{O1}$ and $\text{OW-HW2} \cdots \text{O1}$ hydrogen-bonds generate $R_6^6(24)$ rings [23], while $\text{N1-H1} \cdots \text{OW}$, $\text{OW-HW1} \cdots \text{O1}$, $\text{OW-HW2} \cdots \text{O1}$ and $\text{C11-H11} \cdots \text{Cl1}$ hydrogen bond combinations generate $R_6^6(32)$ rings [23]. In addition, the $\text{C11-H11} \cdots \text{Cl1}$ hydrogen bonds generate $\text{C}(10)$ chains [23] of molecules aligned in the direction of the b axis. Table 4 lists details of the symmetry operations and geometric parameters for these hydrogen bonds.

In $[5 \cdot (\text{H}_2\text{O})]$, strong $\text{N1-H1} \cdots \text{OW}$, $\text{OW-HW1} \cdots \text{O1}$ and $\text{OW-HW2} \cdots \text{O2}$ hydrogen bonds link the molecules of **5** and water into double chains of centrosymmetric rings, [$R_4^4(16)$ $R_4^4(24)$], $C_2^2(14)$ [23], see Fig. 6. The $R_4^4(16)$ rings are formed from

$\text{N1-H1} \cdots \text{OW}$ and $\text{OW-HW1} \cdots \text{O1}$ hydrogen bonds and the $R_4^4(24)$ rings from $\text{OW-HW1} \cdots \text{O1}$ and $\text{OW-HW2} \cdots \text{O2}$ hydrogen bonds. These double chains, formed by the strong and classical $\text{N-H} \cdots \text{O}$ and $\text{O-H} \cdots \text{O}$ hydrogen bonds, are termed strong double chains, to differentiate from other double chains discussed below. Links between these strong double chains are formed by weaker $\text{C2-H2} \cdots \text{O1}$ hydrogen bonds, thereby producing other double chains, termed weaker double chains. This involvement of the $\text{C-H} \cdots \text{O}$ hydrogen bonds, as shown in Fig. 7, generates an alternating sequence of centrosymmetric rings [$R_2^2(10)$], and $R_6^6(30)$ rings [23]: the latter formed from combinations of $\text{C2-H2} \cdots \text{O1}$, $\text{C1-H1} \cdots \text{OW}$ and $\text{OW-HW2} \cdots \text{O2}$ hydrogen bonds, as shown in Fig. 7. Additionally there are short contacts between the double chains involving H6 and O3 [$\text{H6-O3} = 2.61 \text{ \AA}$; $\text{C6} \cdots \text{O3} = 3.530 \text{ \AA}$; $\text{C6-H6} \cdots \text{O3} = 172^\circ$]. However the 2.61 \AA distance is outside the cut-off value for $\text{H} \cdots \text{O}$ separations in $\text{C-H} \cdots \text{O}$ hydrogen bonds [2.50 \AA] and, at best, this indicates a very weak interaction. Table 4 lists details of the symmetry operations and geometric parameters for these hydrogen bonds.

Other intermolecular interactions present in all three hydrates are $\pi \cdots \pi$ stacking [21] and $\text{C-H} \cdots \pi$ [20] interactions, see Table 4 and are illustrated in Fig. 8. The situations for $[3 \cdot (\text{H}_2\text{O})]$ and $[4 \cdot (\text{H}_2\text{O})]$ are similar, but that for $[5 \cdot (\text{H}_2\text{O})]$ is somewhat different.

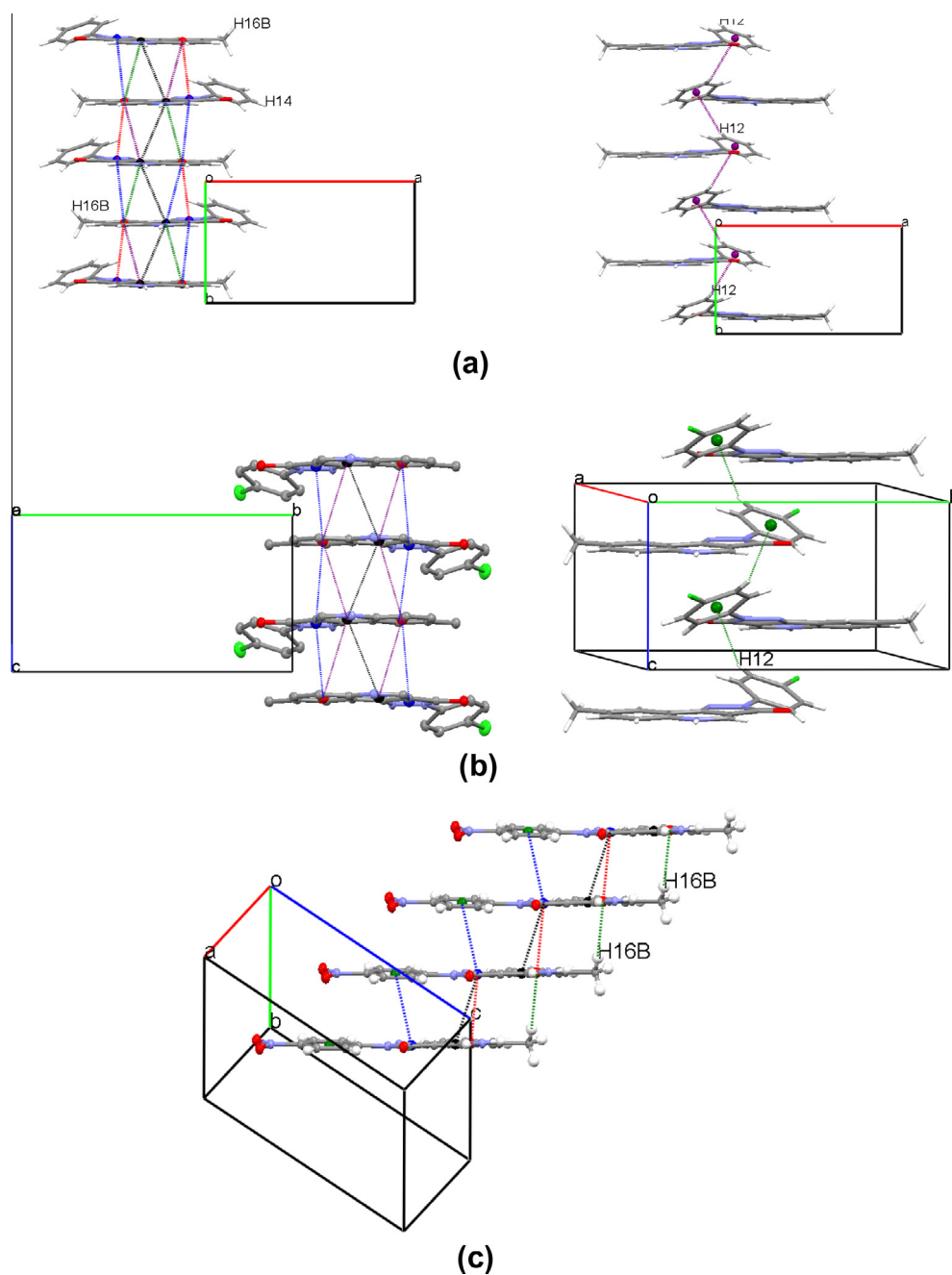


Fig. 8. Stacking and C—H... π interactions in (a) [3·(H₂O)], (b) [4·(H₂O)] and (c) [5·(H₂O)].

In the cases of [3·(H₂O)] and [4·(H₂O)], the stacks of phenylpyrazolo[4,3-*c*]quinolin-3-one molecules are generated from $\pi_{(1)} \cdots \pi_{(3)}$, $\pi_{(2)} \cdots \pi_{(2)}$ and $\pi_{(2)} \cdots \pi_{(3)}$ interactions, where $\pi_{(1)}$, $\pi_{(2)}$ and $\pi_{(3)}$ refer to the diazole, pyridine and phenyl rings of the quinolin-3-one fragment, respectively. Furthermore in both cases, links between the $\pi \cdots \pi$ stacks are generated from C14—H14... $\pi_{(\text{phenyl})}$ interactions. As seen in Fig. 8a and b, the molecules in the stacks alternate in a head-to-toe manner.

In [5·(H₂O)], the $\pi \cdots \pi$ stacks of phenylpyrazolo[4,3-*c*]quinolin-3-one molecules are generated from $\pi_{(1)} \cdots \pi_{(2)}$, $\pi_{(1)} \cdots \pi_{(3)}$ and $\pi_{(1)} \cdots \pi_{(4)}$ interactions, where $\pi_{(1)}$, $\pi_{(2)}$ and $\pi_{(4)}$ refer to the diazole and pyridine phenyl rings of the quinolin-3-one fragment, and the nitrophenyl ring, respectively. Unlike in [3·(H₂O)] and [4·(H₂O)], the C—H... π interactions, specifically C16—H16B... $\pi_{(2)}$ interactions, occur within the stacks and not between them, see Fig. 8c.

As can be seen in Fig. 8c, the molecules in the stacks are off set but are all aligned in the same direction.

The combined intermolecular interactions in all three cases generate three-dimensional arrays.

3.4. Calculations

Calculations were also carried out on several sub-structures, with the initial structures taken as those found in the X-ray study. Single point calculations were carried out on the {[3]₃·(H₂O)}, {[4]₃·(H₂O)} and {[5]₃·(H₂O)} sub-structures, determined in the X-ray study and as illustrated in Fig. 3. As the {[X]₃·(H₂O)} systems were not rigid and as the optimization led to deformations from the initial X-ray derived structures, single point calculations were adopted, rather than full-geometry optimization as the single point

calculations provided the electronic energy without changing the initial atom positions. The stabilizations of the $\{[X]_3 \cdot (H_2O)\}$ aggregates compared to the three molecules of **X** and one water molecule were calculated to be -32.0 , -26.3 and -31.0 kcal mol $^{-1}$, respectively for **X** = **3**, **4** and **5**.

Another calculation was carried out on $\{[5] \cdot (H_2O)_3\}$ substructures. As illustrated in Fig. 3c and described above in Section 3.3, the molecule **5** is bound to three water molecules in a different fashion compared to both molecules **3** and **4** in their $\{[X] \cdot (H_2O)_3\}$ sub-structures. Calculations indicated that the sub-structure determined in the X-ray study for $\{[5] \cdot (H_2O)_3\}$ was more stable, by -7.9 kcal mol $^{-1}$, than that obtained with the three water molecules attached to **5** as in $\{[X] \cdot (H_2O)_3\}$ (**X** = **3** or **4**).

4. Conclusions

The tautomeric form exhibited by the 2-phenylpyrazolo[4,3-c]quinolin-3-one derivatives in the hydrates is invariably form **I**, as was also found for the previous reported anhydrous derivatives, **1** and **2**, and was also calculated in this study. There are only minor differences between the conformations of the 2-phenylpyrazolo[4,3-c]quinolin-3-one molecules in the hydrated and anhydrous compounds. While the water molecules are H-bonded to **3** and **4** via the pyridinyl N and 2 x the carbonyl O atoms, in $\{[5] \cdot (H_2O)\}$ the H-bonds are to pyridinyl N, carbonyl O and a nitro O atoms. Calculations indicated that the found arrangement in $\{[5] \cdot (H_2O)\}$ is more stable than one using the connections as found in $\{[3] \cdot (H_2O)\}$ and $\{[4] \cdot (H_2O)\}$.

As expected the supramolecular arrangements in $[3 \cdot (H_2O)]$, $[4 \cdot (H_2O)]$ and $[5 \cdot (H_2O)]$ differ greatly from those in anhydrous **1** and **2** [9]. In **1** and **2**, the strongest intermolecular interactions, N—H \cdots O_{carbonyl} hydrogen bonds, augmented by weaker C—H \cdots O and $\pi \cdots \pi$ interactions, directly link molecules. In $[3 \cdot (H_2O)]$, $[4 \cdot (H_2O)]$ and $[5 \cdot (H_2O)]$, the strongest interactions, N—H \cdots O and O—H \cdots O hydrogen bonds, link the 2-phenylpyrazolo[4,3-c]quinolin-3-one molecules indirectly via the hydrate molecules, while direct links between the 2-phenylpyrazolo[4,3-c]quinolin-3-one are generated from weaker interactions, such as C—H \cdots π and $\pi \cdots \pi$ interactions. There are differences in the supramolecular arrangements of $[3 \cdot (H_2O)]$ and $[4 \cdot (H_2O)]$, on one hand, with that of $[5 \cdot (H_2O)]$, on the other, due predominantly to the involvement of the nitro group oxygens in strong OW—HW \cdots O_{nitro} hydrogen bonds.

Acknowledgments

The use of the NCS X-ray crystallographic service at Southampton and the valuable assistance of the staff there are gratefully acknowledged. JLW thanks CNPQ for support.

Appendix A. Supplementary material

Full details of the crystal structure determinations in CIF format have been deposited with the Cambridge Crystallographic Data Centre with deposition numbers 937219, 937220 and 937221, respectively for $[3 \cdot (H_2O)]$, $[4 \cdot (H_2O)]$, and $[5 \cdot (H_2O)]$. Copies of these

can be obtained free of charge on written application to CCDC, 12 Union Road, Cambridge, CB2 1EZ, UK (fax: +44 1223 336033); on request by e-mail to deposit@ccdc.cam.ac.uk or by access to <http://www.ccdc.cam.ac.uk>. Supplementary data associated with this article can be found, in the online version, at <http://dx.doi.org/10.1016/j.molstruc.2013.08.032>.

References

- [1] S. Paul, M. Gupta, R. Gupta, A. Loupy, *Tetrahedron Lett.* 42 (2001) 3827–3829.
- [2] P. Smirnov, R.R. Crenshaw, *Antimicrob. Agents Chemother.* 11 (1977) 571–573.
- [3] R.G. Stein, J.H. Beil, T. Singh, *J. Med. Chem.* 13 (1970) 153–155.
- [4] M.R.P. de Oliveira, T.R.A. Alves, A.C. Pinto, H.S. Pereira, L.R. Leão-Ferreira, N. Moussatche, I.C.P.P. Frugulhetti, V.F. Ferreira, M.C.B.V. de Souza, *Nucleos. Nucleot. Nucl. Acids* 23 (2004) 735–748.
- [5] R.I. Fryer, P. Zhang, R. Rios, Z.Q. Gu, A.S. Basile, P. Skolnick, *J. Med. Chem.* 36 (1993) 1669–1673.
- [6] A. Carotti, C. Altomare, L. Savini, L. Chiasserini, C. Pellerano, M.P. Mascia, E. Maciocco, F. Busonero, M. Mameli, G. Biggio, E. Sannac, *Bioorg. Med. Chem.* 11 (2003) 5259–5272, and earlier parts.
- [7] J. Karolak-Wojciechowska, J. Lange, W. Ksiażczka, M. Gniewosz, S. Rump, *Il Farmaco* 53 (1998) 579–585.
- [8] H.O. Villar, M.F. Davies, G.H. Loew, P.A. Maguire, *Life Sci.* 48 (1991) 593–602; W. Zhang, K.F. Koehler, P. Zhang, J.M. Cook, *Drug Des. Discov.* 12 (1995) 124–193; S. Takada, H. Shindo, T. Sasatani, A. Matsushita, M. Eigyo, K. Kawasaki, S. Murata, *J. Med. Chem.* 30 (1987) 454–455; H. Shindo, S. Takada, S. Murata, M. Eigyo, A. Matsuhita, *J. Med. Chem.* 32 (1989) 1213–1217.
- [9] V. Ferretti, V. Bertolasi, G. Gilli, P.A. Borea, *Acta Crystallogr.* C41 (1985) 107–110.
- [10] G.F. Duffin, J.D. Kendall, *J. Chem. Soc.* (1948) 893; C.C. Price, R.M. Roberts, *J. Am. Chem. Soc.* 68 (1946) 1204–1208; M. Khan, F. Pedrotti, *Monatsh Chem.* 113 (1982) 123–127; M.S. Puar, P.T. Funke, A.I. Cohen, *J. Pharm. Sci.* 67 (1978) 850–853.
- [11] M.J. Frisch, G.W. Trucks, H.B. Schlegel, G.E. Scuseria, M.A. Robb, J.R. Cheeseman, G. Scalmani, V. Barone, B. Mennucci, G.A. Petersson, H. Nakatsuji, M. Caricato, X. Li, H.P. Hratchian, A.F. Izmaylov, J. Bloino, G. Zheng, J.L. Sonnenberg, M. Hada, M. Ehara, K. Toyota, R. Fukuda, J. Hasegawa, M. Ishida, T. Nakajima, Y. Honda, O. Kitao, H. Nakai, T. Vreven, J. A. Montgomery, Jr., J.E. Peralta, F. Ogliaro, M. Bearpark, J.J. Heyd, E. Brothers, K.N. Kudin, V.N. Staroverov, T. Keith, R. Kobayashi, J. Normand, K. Raghavachari, A. Rendell, J.C. Burant, S.S. Iyengar, J. Tomasi, M. Cossi, N. Rega, J.M. Millam, M. Klene, J.E. Knox, J.B. Cross, V. Bakken, C. Adamo, J. Jaramillo, R. Gomperts, R.E. Stratmann, O. Yazyev, A.J. Austin, R. Cammi, C. Pomelli, J.W. Ochterski, R.L. Martin, K. Morokuma, V.G. Zakrzewski, G.A. Voth, P. Salvador, J.J. Dannenberg, S. Dapprich, A.D. Daniels, O. Farkas, J.B. Foresman, J.V. Ortiz, J. Cioslowski, D.J. Fox, *Gaussian 09, Revision D.01*, Gaussian, Inc., Wallingford, CT, 2013.
- [12] R.W.W. Hooft, COLLECT, Data Collection Software, Nonius BV, Delft, The Netherlands, 1998.
- [13] Z. Otwinowski, W. Minor, *Processing of X-ray diffraction data collected in oscillation mode*, in: C.W. Carter Jr., R.M. Sweet (Eds.), *Macromolecular Crystallography, Part A. Methods in Enzymology*, vol. 276, Academic Press, New York, 1997, pp. 307–326.
- [14] CrystalClear-SM Expert, Rigaku Corporation, Tokyo, Japan, 2011.
- [15] G.M. Sheldrick, G.M. SADABS Version 2007/2, Bruker AXS Inc., Madison, Wisconsin, USA, 2007.
- [16] L.J. Farrugia, *J. Appl. Crystallogr.* 32 (1999) 837–838.
- [17] Mercury 3.0, Cambridge Crystallographic Data Centre, UK.
- [18] G.M. Sheldrick, *Acta Crystallogr.* A64 (2008) 112–122.
- [19] A.L. Spek, *J. Appl. Crystallogr.* 36 (2003) 7–13.
- [20] M. Nishio, *CrystrEngChem* 6 (2004) 130–158.
- [21] C.A. Hunter, J.K.M. Sanders, *J. Am. Chem. Soc.* 112 (1990) 5525–5534; C.A. Hunter, *Chem Soc. Rev.* (1994) 101–109.
- [22] V.R. Hathwar, S.M.R. Roopan, R. Subashini, F.N. Khan, T.N. Guru Row, *J. Chem. Sci.* 122 (2010) 677–685.
- [23] J. Bernstein, R.E. Davies, L. Shimoni, N.-L. Chang, *Angew. Chem. Int. Ed. Engl.* 34 (1995) 1555–1573.